Advantages of Covalent Immobilization of Metal-Salophen on Amino-Functionalized Mesoporous Silica in Terms of Recycling and Catalytic Activity for CO 2 Cycloaddition onto Epoxides

Matthieu Balas, Sébastien Beaudoin, Anna Proust, Franck Launay, Richard Villanneau

EurJIC
European Journal of Inorganic Chemistry

Full Papers
doi.org/10.1002/ejic.202100150

Chemistry Europe
European Chemical Societies Publishing

Advantages of Covalent Immobilization of Metal-Salophen on Amino-Functionalized Mesoporous Silica in Terms of Recycling and Catalytic Activity for CO_2 Cycloaddition onto Epoxides

Matthieu Balas,[a, b] Sébastien Beaudoin,[a, b] Anna Proust,[a] Franck Launay,*[b] and Richard Villanneau*[a]

Dedicated to the memory of Professor Michel Che

Ni^{II} and Mn^{III} Schiff base complexes (Salophen-Ni and Salophen-MnCl) bearing a pending carboxylic group were prepared and characterized. Both complexes were grafted onto a mesoporous amino-functionalized SBA-15 silica, by formation of an amide function between the propylamine groups of the support and the carboxylic acid functions of the salophen ligand (corresponding respective to 1.30 wt.% of Ni and 1.06 wt.% of Mn). The co-catalytic behaviour of the free and grafted complexes was then evaluated in the CO_2 cycloaddition reaction onto styrene oxide, using tetra-butylammonium bromide ($^{n-}Bu_4NBr$) as the main catalyst. In homogeneous conditions, the Mn^{III} Schiff base complex and the Ni^{II} one, to a lesser extent, behave as efficient co-catalysts for this reaction (styrene conversion of 100% and 65% respectively after 3 h at 120 °C, under 15 bars of CO_2). Upon immobilization at the surface of the amino-functionalized SBA-15, we showed that the co-catalytic activity of the less efficient one, i.e. Ni^{2+} salophen complex, could be enhanced (reaching a full conversion after 7 h), hence highlighting a potential synergistic effect between the unused amine functions of the support and the Ni^{2+} salophen co-catalyst. Both salophen complexes were successfully re-used in homogeneous conditions or after their immobilization without any appreciable loss of activity. This work is only a first step towards a completely heterogeneous catalytic system, in which the tetraalkylammonium halide catalyst and the metal-salophen co-catalyst will both be covalently anchored on the same support.

■■■Dear author, please check whether the numbering and hierarchy of the headlines are correct – they were not numbered consistently■■■

1. Introduction

The large amounts of carbon dioxide released to the atmosphere by human activities significantly contribute to the greenhouse effect. In this context, methods using CO_2 as a renewable, abundant C1-source to produce valuable chemicals are regarded with large interest and research concerning CO_2 transformation has led to significant progress.[1–10] In this context, CO_2 coupling reactions with epoxides leading to useful cyclic carbonates[8–14] have attracted particular attention in the community. CO_2 industrial applications already exist but need to be much more developed. Valuable products such as carboxylic acids, carbamates and carbonates can be obtained.[15] In such synthesis, carbon dioxide behaves as a green reagent as the result of its direct reaction with epoxides avoiding the use of phosgene, an extremely toxic reagent, and the formation of by-products.[16] Ethylene and propylene carbonates are already obtained at industrial scale by the reaction of CO_2 with epoxides in the presence of organocatalysts such as quaternary ammonium (NR_4^+, X^-) or phosphonium (PR_4^+, X^-) salts (mainly halogenated ones). Reaction conditions are however severe with temperatures and pressures of 120 °C and 40 bar, respectively.[17] According to recent studies, milder conditions can be used when quaternary ammonium salts (QAS) are combined with co-catalysts,[8–14,18–27] generally hydrogen bond donor compounds[8–10] or metal complexes.[11–14] The latter provide Lewis acidity and thus, facilitate the nucleophilic attack of the activated epoxide by counter-anions of QAS. In this regard, transition metal complexes (especially Schiff bases and porphyrins complexes) are particularly promising.[28–29] Salen-type compounds have been introduced very early by North[18] and Zhang,[19] then porphyrins by Ema[30] and, more recently, Schiff bases with 4 nitrogen atoms

[a] M. Balas, S. Beaudoin, Prof. A. Proust, Dr. R. Villanneau
Sorbonne Université, CNRS, Campus Pierre et Marie Curie
Institut Parisien de Chimie Moléculaire, CNRS UMR 8232
4 Place Jussieu, 75005 Paris, France
E-mail: richard.villanneau@sorbonne-universite.fr
http://www.ipcm.fr/villanneau-richard
[b] M. Balas, S. Beaudoin, Prof. F. Launay
Sorbonne Université, CNRS, Campus Pierre et Marie Curie
Lab. de Réactivité de Surface, CNRS UMR 7197
4 Place Jussieu, 75005 Paris, France
E-mail: franck.launay@sorbonne-universite.fr
http://www.lrs.upmc.fr/en/personal-page-of-researchers/franck-launay.html

Supporting information for this article is available on the WWW under https://doi.org/10.1002/ejic.202100150

(BS4N) by Christ and Masdeu-Bulto.[28] Some of the systems involving metal complexes and QAS operate at room temperature and at atmospheric pressure.[31] In recent years, significant advances have led to a great reduction of the catalyst loading, particularly of the QAS. In parallel, several studies on the use of efficient co-catalysts immobilized on supports using a more or less sophisticated pathway have emerged in the literature.[32–39] In the light of our recent studies dealing with the immobilization of polyoxometalates on mesoporous supports,[40–41] the present work focuses on the covalent grafting of Ni and Mn metal-salophen complexes bearing a carboxylic acid group onto propylamine-functionalized mesoporous silica of the SBA-15 type (Figure 1). In particular, the strategy developed allowed the straightforward immobilization of the metal-salophen co-catalysts onto the inorganic support, and, the comparison of their reactivity for the CO_2 cycloaddition onto styrene oxide, in homogeneous and heterogeneous conditions.

2. Results and Discussion

Here, in continuity with our previous work[40–41] on metal complexes immobilization, the strategy used consisted in the coupling of complementary functions, one (amino group) at the oxide support (amino group) and the second at the termination of the organic salophen ligand. To do so, two different metal complexes (with either Ni^{II} or $\{Mn^{III}–Cl\}^{2+}$) were prepared with a salophen ligand bearing a remote carboxylic acid function. Comparison of the co-catalytic reactivity of the two complexes in solution and after their immobilization was performed for the cycloaddition of CO_2 onto styrene oxide in the presence of $^{n-}Bu_4NBr$ for the preparation of styrene carbonate.

2.1. Synthesis and characterization of the ligand H_2Salophen and of its Ni(II) and Mn(III) complexes

A convenient salophen ligand that meets all the criteria is N,N′-bis(3,5-di-tert-butylsalicylidene)-1-carboxy-3,4-phenylene-diamine, denoted H_2Salophen (**1**, Figure 2) whose synthesis, in the present study, was adapted from the literature.[42]

Hence, the Schiff-base ligand **1** was synthesized with 95 % yield (see SI for the details of the preparation) using a classical condensation reaction of 1,2-diamino-4-carboxybenzene with 2 equivalents of 3,5-di-*tert*-butyl-2-hydroxybenzaldehyde (3,5-di-*tert*-butylsalicylaldehyde). It is noteworthy that this reaction required the presence of Zn^{2+} that played the dual role of a templating agent and a Lewis acid that was not recovered in the final product. The ligand **1** was characterized in mass spectrometry (HRMS) by a molecular peak at m/z ($[M+H]^+$) = 585.37 (Figure S1). The ^{1}H NMR spectrum (Figure S2) was consistent with the literature[42–43] showing several characteristic peaks, among which two groups of singlets were attributed respectively to the imine functions (–HC=N– at 9.08 and 9.02 ppm) and the phenol groups (13.69 and 13.61 ppm). The formation of the imine functions was also attested in IR spectroscopy by the absence of the $\nu_{(NH2)}$ bands of the initial 1,2-diamino-4-carboxybenzene at 3400 and 3487 cm^{-1} and by the occurrence of the $\nu_{(–HC=N–)}$ band at 1686 cm^{-1}.

Many transition metal complexes with Schiff-Base ligands were used in the literature for the CO_2 cycloaddition onto epoxides. In the present work, we focused our attention on Ni^{2+} and Mn^{3+} complexes. While many examples of co-catalysts based on Mn^{3+} salen/salophen/porphyrin complexes have been reported,[44–47] those based on Ni^{2+} are scarce.[48] Furthermore, the Salophen-Ni (**2**) complex obtained by reaction of ligand **1** with $NiCl_2.6H_2O$ displays a square planar geometry in which the Ni^{2+} ion was found diamagnetic. It was thus possible to characterize complex **2**, in contrast to the Mn one, by ^{1}H NMR spectroscopy in solution, but also by ^{13}C CP-MAS NMR spectroscopy in view of its subsequent immobilization.

In the case of the Salophen-Ni (**2**) complex synthesis, the procedure described in the literature was significantly modified. Indeed, the synthesis reported by Hey-Hawkins and co-workers was a *one-pot* reaction from the starting reagents (1,2-diamino-4-carboxybenzene and 3,5-di-*tert*-butylsalicylaldehyde) in the presence of a Ni^{2+} source replacing the

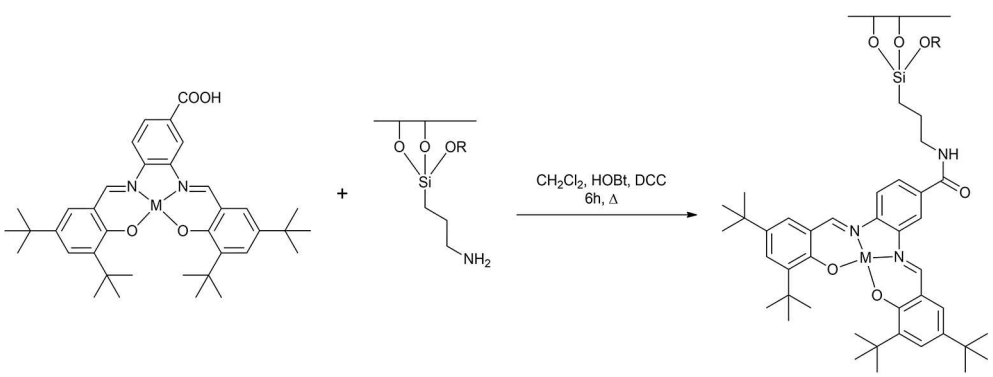

Figure 1. Covalent grafting strategy to anchor metal-salophen (N,N′-bis(3,5-di-tert-butylsalicylidene)-1-carboxy-3,4-phenylene-diamine) complexes onto propylamine-functionalized SBA-15 silica (HOBt = 1-hydroxy-1H-benzotriazole; DCC=*N,N′*-dicyclohexylcarbodiimide).

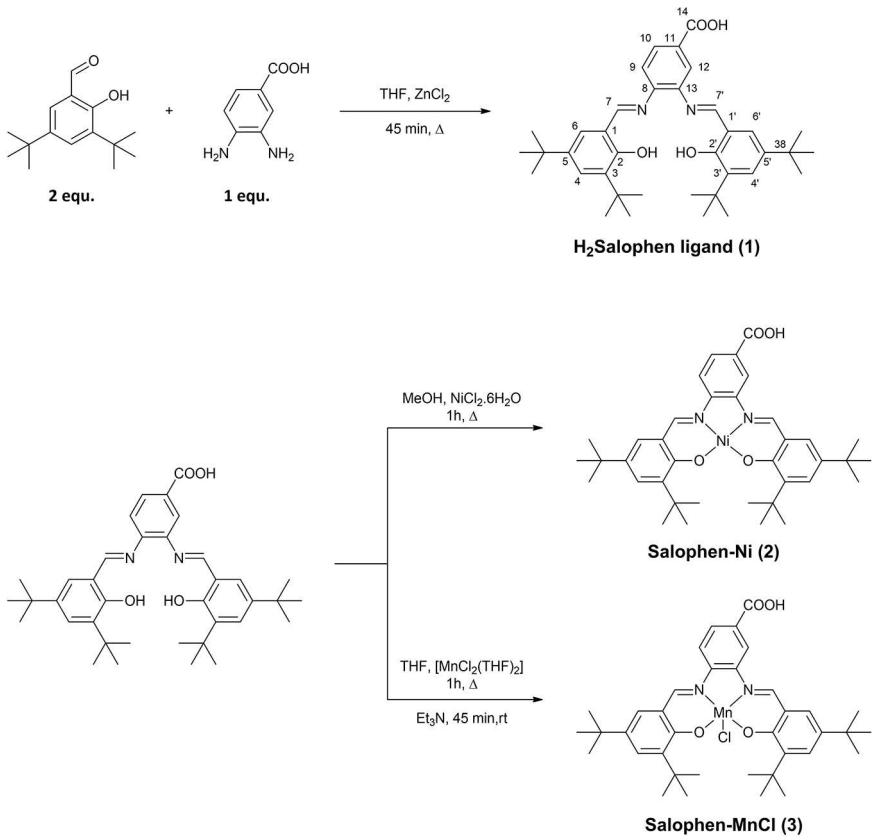

Figure 2. Routes synthesis of N,N′-bis(3,5-di-tert-butylsalicylidene)-1-carboxy-3,4-phenylene-diamine (H_2Salophen ligand **1**, top) and its complexation leading to Salophen-Ni (2) and Salophen-MnCl (3).

templating Zn^{2+} ion[42]. However, we found that his procedure led to low yields and to mixtures of different reaction products. We thus turned to the direct complexation of Ni^{2+} ions by the non-metallated ligand **1** in dry methanol. This procedure, which was also used for the complexation of Mn^{3+}, finally led to 51 and 88% yield of Salophen-Ni (**2**) and Salophen-MnCl (**3**), respectively with high purity, as attested by HRMS (Figure S4 and Figure S5) and ^{1}H NMR (for the salophen-Ni (**2**), Figure S3). In the Salophen-MnCl complex (**3**), the Mn^{3+} displays a square pyramid five-coordination, the coordination sphere being completed with a chloride anion. Complexes **2** and **3** were characterized in mass spectrometry (HRMS) by a molecular peak respectively at m/z ($[M–H]^-$) = 639.27 for the salophen-Ni **2** (Figure S4) and at m/z ($[M–Cl]^+$) = 637.28 for the Salophen-MnCl **3** (Figure S5), in accordance with the literature.[42]

The ^{1}H NMR spectrum of Salophen-Ni (**2**) (Figure S3) confirmed its diamagnetism. We did not observe any broadening of the peaks, as expected in the case of a paramagnetic system. It is noteworthy that the two singlets assigned to the –OH groups of ligand **1** were not found in the spectrum of complex **2**, thus confirming the complexation of Ni^{2+} by the oxygen of the two phenol groups. Furthermore, the Ni complexation was emphasized by the shift of all the peaks of the salophen ligand in comparison with those of the free ligand **1**.

2.2. Synthesis and characterization of {NH_2}–SBA-15 and of the covalently immobilized Ni^{2+} (2) and Mn^{3+} (3) catalysts

The amino-functionalized SBA-15 (for short {NH_2}–SBA-15) was obtained by the functionalization of a pre-formed SBA-15 silica[49] with 3-aminopropyltriethoxysilane (Scheme S1), as described previously, targeting 4 mmol g^{-1}.[50–51] The thermogravimetric curve of {NH_2}–SBA-15 (Figure 3) obtained under air from room temperature up to 700 °C shows two weight losses. The first one (*ca.* 3%), under 100 °C (not shown here), can be attributed to the loss of water molecules weakly adsorbed on the silica surface whereas the second one (13%, 100–600 °C) was assigned to the loss of aminopropyl functions. This analysis demonstrated that {NH_2}–SBA-15 is functionalized with 2.3 mmol of {NH_2} g^{-1} (*c.a.* 58% incorporation yield). The general formula of {NH_2}–SBA-15 is then $H_2N(CH_2)_3Si/5.8SiO_2$.

The covalent immobilization of Mn^{3+} Salen complexes onto an organically modified silica surface was previously described in the literature.[42–47,52] However, the grafting procedures in all these examples generally required a multi-step functionalization of the hybrid support and/or of the salen ligands, which does not meet the criteria for the development of sustainable catalytic processes. The grafting procedure of the two complexes in the present study was inspired by the work of Luts and Papp[43] and by our previous

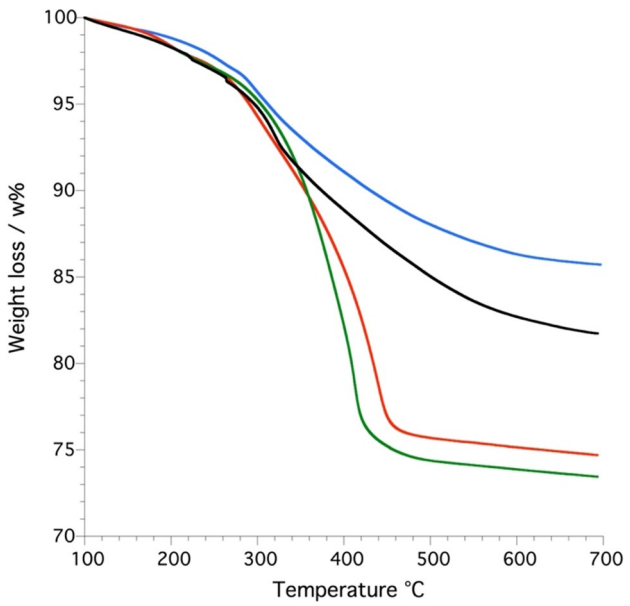

Figure 3. Weight loss % (thermogravimetric analysis, TGA) for {NH2}–SBA-15 (blue), Salophen-Ni/{NH2}–SBA-15 (sample without coupling agent) (black), Salophen-Ni@{NH2}–SBA-15 (green), Salophen-MnCl@{NH2}–SBA-15 (red). All the curves were normalized at 100 °C.

studies on the heterogenization of hybrid derivatives of polyoxometalates onto {NH_2}–SBA-15.[41] In these two examples, the strategy of linkage was built on the functionalization of both the catalyst and the mesoporous silica support by complementary organic functions leading to the formation of robust and non-hydrolyzable amide groups. This choice is justified both by the efficiency and convenience of grafting aminopropyl synthons onto the SiO_2 support and by the one-step preparation of the salophen ligand from commercial reagents. In the present work, the formation of an amide function by reaction between the carboxylic acid of the salophen ligand in complexes **2** and **3** and the aminopropyl functions of the {NH_2}–SBA-15 support was realized using N,N′-dicyclohexylcarbodiimide (DCC) and 1-hydroxy-1H-benzotriazole (HOBT), in dichloromethane under refluxing conditions (–CO_2H:1, HOBT:0.3, DCC:1.4 and –NH_2 4.3 for Salophen-Ni@{NH_2}–SBA-15 or 7.7 for Salophen-MnCl@{NH_2}–SBA-15). After each synthesis, the two materials thus obtained (Salophen-Ni@{NH_2}–SBA-15 and Salophen-MnCl@{NH_2}–SBA-15) were then extracted in a soxhlet and washed for 3 days successively with methanol and acetone to remove all the physisorbed complexes. It is noteworthy that these grafting and washing protocols were optimized in our previous work with polyoxometalates.[41] Indeed, our past studies showed that these steps are crucial to obtain materials in which the active phases are effectively covalently grafted in order to avoid later any leaching/lixiviation phenomenon. Finally, it should be noted that, after the soxhlet treatment, the color of the samples remained dark (dark brown with Mn and red/purple for Ni).

The weight percentages of Ni and Mn in Salophen-Ni@{NH_2}–SBA-15 and Salophen-MnCl@{NH_2}–SBA-15, respectively were determined by Atomic Absorption measurements (see details in SI). These amounts are important and comparable in both materials, 1.30 wt.% of Ni in Salophen-Ni@{NH_2}–SBA-15 and 1.06 wt.% of Mn in Salophen-MnCl@{NH_2}–SBA-15, corresponding to grafting yields respectively equal to 52% (Ni) and 68% (Mn) regarding the initial Ni or Mn loadings. Such values were confirmed indirectly by thermogravimetric analyses (TGA, Figure 3). Indeed, it was possible to get a reasonable estimation of the effective amount of Salophen-Ni/Mn in the final materials by subtracting the loss weight of the propylamine functions present in the starting {NH_2}–SBA-15 (see details in SI). The wt.% of Ni or Mn in the materials was estimated to 1.30 and 1.03% respectively, in good accordance with the results of the atomic absorption measurements. This corresponds to 0.22 mmol of Ni^{2+} per gram of Salophen-Ni@{NH_2}–SBA-15 and 0.19 mmol of $\{MnCl\}^{2+}$ per gram of Salophen-MnCl@{NH_2}–SBA-15. It is noteworthy that the initial Ni^{2+}/{–NH_2} functions and $\{MnCl\}^{2+}$/{–NH_2} functions ratios described in the experimental part correspond to optimized conditions for both systems. In other words, an increase or a decrease of these ratios did not allow an increase of Ni^{2+} or $\{MnCl\}^{2+}$ loadings in the final materials.

In order to evaluate the efficiency of the covalent grafting of the complexes onto the surface, a blank test was done in which the deposition of the Salophen-Ni (**2**) was carried out in the absence of a coupling agent (DCC and HOBT). This test was performed with experimental conditions (concentrations, temperature, duration of the experiment and work up) similar to those used in the presence of the coupling agent. After the washing step (4 days using a soxhlet in methanol and acetone), this control sample was visually different as the resulting solid had a light red color. TGA analyses, displayed on Figure 3, were also performed on this sample for sake of comparison. As expected, the amount of Salophen-Ni was found significantly lower in the absence of the coupling agents ($Ni\%_{weight} = 0.40\%$). When DCC and HOBT are used, all these data led us to envisage a strong linkage of the Salophen-Ni/MnCl complexes with silica in Salophen-Ni@{NH_2}–SBA-15 and Salophen-MnCl@{NH_2}–SBA-15 that differs clearly from a simple physical adsorption. This also shows that this protocol is relevant as regards the immobilization of this type of co-catalyst. Therefore, it validates in a more general way our covalent grafting strategy on mesoporous support 1) to limit the lixiviation phenomena during subsequent catalytic tests and 2) to increase the loading rate of the metal-salophen complexes in the catalytic materials.

The ^{13}C CP-MAS NMR spectrum of complex **2** in its solid state showed a large number of peaks (Figure S6) due to its low symmetry and the absence of free rotation of the methyl groups of the $^{t-}$butyl functions (up to 37 non-equivalent carbon atoms). Despite a lower resolution of the spectrum of Salophen-Ni@{NH_2}–SBA-15 compared to the spectrum of **2**, similar patterns were observed for both samples (Figure S6). In particular, the most intense peak at 31.2 ppm (assigned to

some methyl of the ^{t}–butyl groups of the salophen) was clearly observed in both samples. In addition, it is noteworthy that the spectrum of Salophen-Ni@{NH_2}–SBA-15 was dominated by the three peaks (topped with an asterisk) attributed to the carbon atoms of the propylamine functions of the support.

The Raman spectra of the Salophen-Ni and Salophen-MnCl complexes in solid state were also compared to those of Salophen-Ni@{NH_2}–SBA-15 (Figure 4) and Salophen-MnCl@{NH_2}–SBA-15, respectively (Figure 5). In both cases, the two datasets clearly indicated that the spectroscopic footprints of the supported complexes are identical to those of the pure complexes in the solid state. This confirmed that the integrity of both complexes was maintained after surface grafting, even though the spectrum of Salophen-MnCl@{NH_2}–SBA-15 was less well defined, probably due to fluorescence phenomena under Raman beam. It is noteworthy that Raman spectra of Base-Schiff compounds are complex, displaying many bands and consequently are difficult to index in detail. However, by comparison with the data obtained on the parent complex without ^{t}–Butyl and carboxylic groups (*i.e.* N,N′-bis(salicylaldehyde)-1,2-phenylenediamine-nickel(II)),[53–54] it was possible to identify and assign the most intense bands at 1412 ($\delta_{HC=N}$) and 1573 cm^{-1} ($\nu_{C=C}$ aromatic) on the spectra of both the Salophen-Ni and the Salophen-MnCl complexes.

The Salophen-Ni@{NH_2}–SBA-15 and Salophen-MnCl@{NH_2}–SBA-15 materials were also characterized by High-Resolution Transmission Electronic Microscopy (HR-TEM), after microtome cutting (Figure 6 and Figure 7). For both samples, the micrographs showed that the grafting of the Salophen complexes did not alter the porosity of the support.

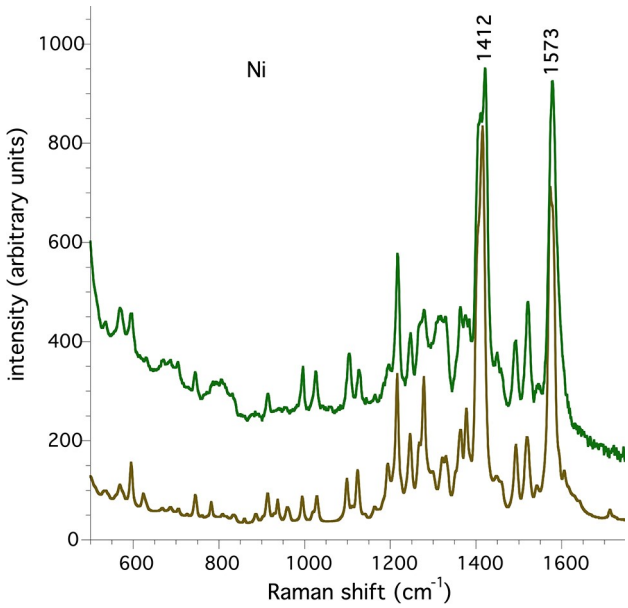

Figure 4. Raman spectra of Salophen-Ni (**2**) (in brown) and Salophen-Ni@{NH_2}–SBA-15 (in green).

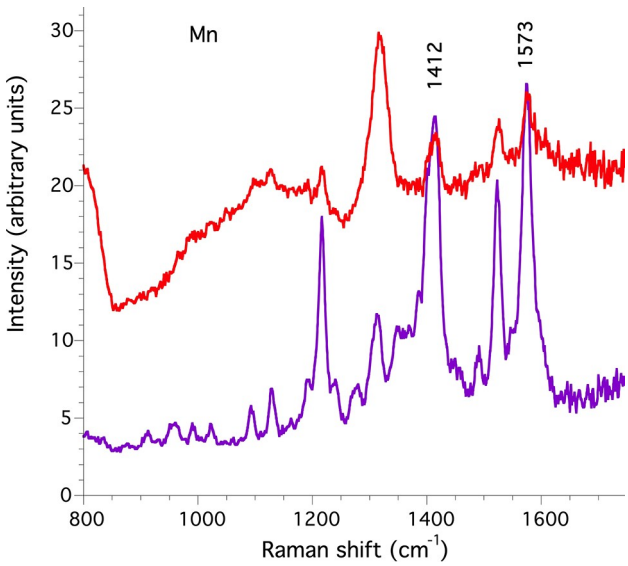

Figure 5. Salophen-MnCl (**3**) (in purple) and Salophen-MnCl@{NH_2}–SBA-15 (in red).

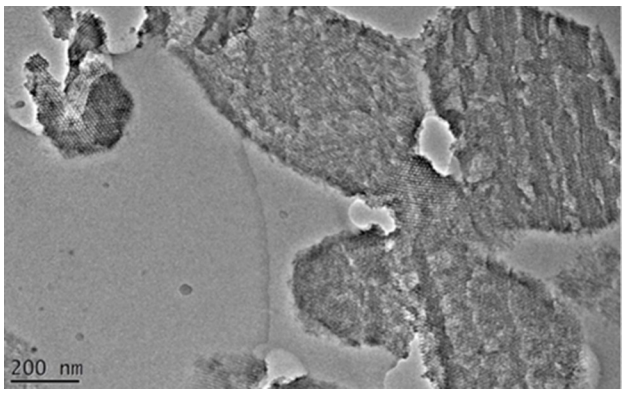

Figure 6. HR-TEM micrograph of Salophen-Ni@{NH2}–SBA-15 after microtome cutting.

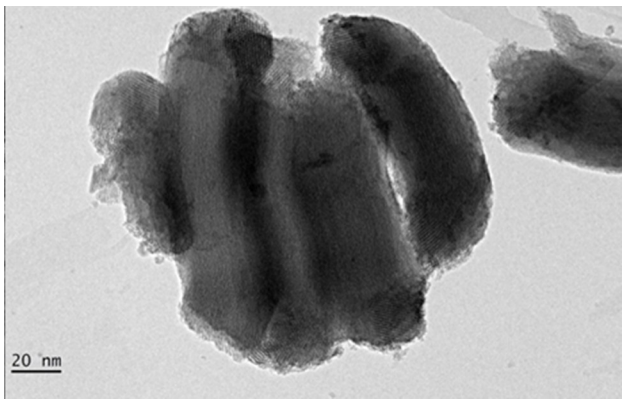

Figure 7. HR-TEM micrograph of Salophen-MnCl@{NH2}–SBA-15 after microtome cutting.

The N_2 adsorption-desorption isotherms of the SBA-15-based materials (Figure 8) exhibited characteristic type IV patterns with H_1 hysteresis confirming that all materials were constituted of mesoporous channels of relatively uniform diameter.

The pore properties of the materials at the different stages of their preparation were determined from their nitrogen adsorption-desorption isotherms using the Brunauer-Emmet-Teller (BET) and the Barret-Joyner-Halenda (BJH) models (Table 1).

As expected, the textural parameters of the mesoporous materials significantly decreased after each functionalization step: the final BET specific surface areas were respectively 350 $m2.g^{-1}$ for for Salophen-Ni@{NH2}–SBA-15 and 300 $m2.g^{-1}$ for Salophen-MnCl@{NH2}–SBA-15 (see Figure S7). However, this remains compatible with their utilization in anchored homogeneous catalysis.

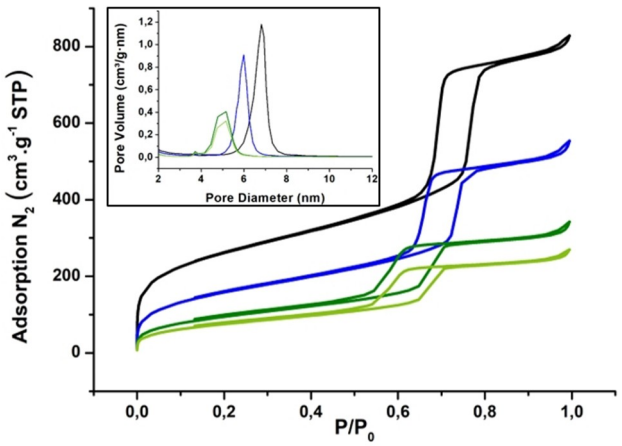

Figure 8. Nitrogen adsorption-desorption isotherms (77 K) of SBA-15 (black), {NH_2}–SBA-15 (blue), and Salophen-Ni@{NH_2}–SBA-15 before (dark green) and after 4 catalytic cycles (light green) with pores size distribution curves (inset).

Table 1. Evolution of the textural properties of the materials upon their functionalization.

Sample	S_{BET}[a] [$m^2 g^{-1}$]	Pore vol.[b] [$cm^3 g^{-1}$]	Average pore diameter[b] [nm]
SBA-15	900	1.12	6.2
{NH_2}–SBA-15	530	0.63	5.7
Salophen-MnCl@{NH_2}–SBA-15	300	0.45	5.4
Salophen-Ni@{NH_2}–SBA-15	350	0.48	5.1
Salophen-Ni@{NH_2}–SBA-15 (after 4 catalytic cycles)	280	0.38	5.0

[a] Use of the BET model for $P/P^0 < 0.25$; [b] Use of the BJH model for the treatment of the desorption branch with $2 <$ pore range < 26 nm.

2.3. Comparison of the co-catalytic activity of the Salophen-type complexes in the styrene oxide conversion into styrene carbonate in homogeneous and heterogeneous conditions

2.3.1. Homogeneous conditions

The formation of styrene carbonate from styrene epoxide and CO_2 (Scheme 1) was firstly studied in homogeneous conditions. We thus used for this $^{n-}Bu_4NBr$ and the Ni/Mn–Cl Salophen (2 and 3) complexes respectively as the catalyst and co-catalysts in benzonitrile. The reaction was performed in an autoclave under 15 bars of CO_2 at 120 °C and monitored by Gas-Chromatography and ^1H NMR spectroscopy after 3 h, 7 h and 23 h.

As already reported,[55] a fairly good conversion of styrene oxide was observed with $^{n-}Bu_4NBr$ alone (no metal co-catalysts) after 7 h (81 %, see entry 1 Table 2) using a styrene oxide:$^{n-}Bu_4NBr$ molar ratio of 60. However, the reaction slowed considerably afterwards (84 % after 23 h). Typical experiments were performed with a total volume of liquid phase equal to 14 mL (13.3 mL of benzonitrile and 0.7 mL of styrene oxide) in the 100 mL vessel. It is noteworthy that this corresponds to the optimized reaction conditions, since the yield in styrene carbonate was shown to be significantly dependent on the CO_2 pressure but also on the number of moles of CO_2 available in the vessel. Thus, using the same styrene oxide concentration (0.44 mol L^{-1}) and the same styrene oxide: $^{n-}Bu_4NBr$ (60 : 1) molar ratio, but tripling the

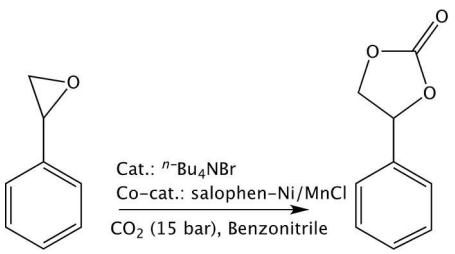

Scheme 1. CO_2 cycloaddition onto styrene oxide.

Table 2. Conversion of styrene oxide into styrene carbonate with homogeneous and supported catalysts.[a]

Entry	Catalyst	Co-catalyst	[%] Styrene conv. 3 [h]	7 [h]	23 [h]
1	$^{n-}Bu_4NBr$	–	62	81	84
2	$^{n-}Bu_4NBr$	Salophen-Ni (**2**)	65	85	100
3	$^{n-}Bu_4NBr$	Salophen-MnCl (**3**)	100	100	100
4	–	Salophen-Ni (**2**)	/	/	0
5	–	Salophen-MnCl (**3**)	/	/	2
6	$^{n-}Bu_4NBr$	Jacobsen catalyst (commercial)	100	100	100
7	$^{n-}Bu_4NBr$	Salophen-Ni@{NH_2}–SBA-15	80	98	100
8	$^{n-}Bu_4NBr$	Salophen-MnCl@{NH_2}–SBA-15	80	100	100
9	$^{n-}Bu_4NBr$	{NH_2}–SBA-15[b]	81	86	98

[a] Conditions: Styrene oxide (6.1 mmol), $^{n-}Bu_4NBr$ (0.1 mmol), homogeneous or supported Salophen-M (0.05 mmol of metal) in 13.3 mL of benzonitrile at 120 °C under 15 bars of CO_2. [b] For experimental details see the Supporting Information.

volume of the solution in the closed vessel, led to a significant decrease in styrene oxide conversion from 81% to 40% after 7 h due to the reduction of the molar excess of CO_2 from 7 to 1.5.

In all experiments, the possible presence of polycarbonates (potentially obtained by co-polymerization of styrene oxide with styrene carbonate) was checked by ^1H and ^{13}C NMR spectroscopy. In any cases, no trace of polymers was detected. This was confirmed by the mass balance determination by GC using mesitylene as an internal standard. Thereafter, considering a selectivity of 100%, the total yield in styrene carbonate was assimilated to the conversion of styrene oxide.

Keeping similar reaction conditions (15 bar of CO_2 at 120 °C and CO_2: epoxide = 7:1) and using metal salophen complexes **2** or **3** as co-catalysts with a co-catalyst: catalyst ratio of 1:2 (Table 2, entries 2 and 3), a complete conversion of styrene oxide could be reached. We have checked that both complexes were not able to catalyse alone the CO_2 cycloaddition onto styrene oxide (Table 2, entries 4 and 5). The rate increase in the presence of salophen complexes was found to be strongly metal dependent. While the gain in the styrene oxide conversion was relatively modest with the Salophen-Ni (**2**) (conversion of 65 and 85% after respectively 3 and 7 h), it was significant after 3 h (100% conversion) in the case of the Mn^{III} derivative (**3**). The styrene carbonate yield obtained with the latter was found to be identical to that obtained with the commercial Mn Jacobsen catalyst (Table 2, entry 6) under the same conditions, which means that the diamine used in the synthesis of the salophen was less critical than the metal. An additional test performed with **3** and $^{n-}Bu_4NBr$ showed actually that, after one hour at 120 °C, the styrene oxide conversion was 96%. Even if the catalytic activity of the *n*-Bu_4NBr/Salophen-Ni (**2**) system in homogeneous conditions is slightly lower than that obtained with *n*-Bu_4NBr/Salophen-MnCl (**3**), it is noteworthy that this result deserved special emphasis since examples of Ni co-catalysts for the CO_2 cycloaddition are scarce.

2.3.2. Heterogeneous conditions

The activity of the two anchored co-catalysts (Salophen-Ni@{NH_2}–SBA-15 or Salophen-MnCl@{NH_2}–SBA-15) was studied in the same reaction conditions (Table 2, entries 7 and 8) with 0.44 M styrene oxide keeping $^{n-}Bu_4NBr$ as a homogeneous catalyst with a styrene oxide: $^{n-}Bu_4NBr$ molar ratio of 60 and using amounts of supported Salophen-Ni (2) or Salophen-MnCl (3) rigorously analogous to those employed in Table 2 (entries 2 and 3) for soluble Salophen-Ni (2) and Salophen-MnCl (3), respectively. With Salophen-Ni@{NH_2}–SBA-15 and Salophen-MnCl@{NH_2}–SBA-15, the results obtained were comparable, allowing near complete conversion of styrene oxide after 7 h. As early as 3 h of reaction, supported Salophen-Ni showed much better performance than its homogeneous counterpart. With both supported complexes, the conversion was 80% after 3 h. Such conversion value for Salophen-MnCl@{NH_2}–SBA-15 corresponds to a slight decrease compared to what was observed for Salophen-MnCl tested in homogeneous conditions (80% conversion after 3 h instead of 100%). Indeed, heterogenized (co-)catalysts are often less active at early stage than their homogeneous counterparts due to diffusion limitations. However, it is somewhat surprising to observe a significant increase in co-catalytic activity after supporting the nickel complex (80% conversion after 3 h instead of 65%). Finally, there are only a few examples of salen complexes covalently immobilised on silica whose catalytic properties have been evaluated in CO_2 cycloaddition in the literature, with mainly Al, Cr, Zn or Mn ions.[33,56–59] To our knowledge, no nickel heterogenized complex was described. As far as manganese complexes are concerned, comparisons are hardly made, as the experimental conditions are very different from one study to another. For instance, silylated Salen-Mn(III) covalently grafted onto silica showed interesting catalytic performances in the absence of tetraalkylammonium halide with a 95% yield in styrene carbonate after 3 h reaction but with very harsh reaction conditions, 140 °C under 35 bar of CO_2.[59]

In order to better understand the differences between the homogeneous and supported Ni co-catalysts, we also investigated the potential co-catalytic activity of the support itself, {NH_2}–SBA-15 keeping $^{n-}Bu_4NBr$ as the main catalyst (Table 2, entry 9, see details in SI). It is indeed necessary to have in mind that Salophen-Ni@{NH_2}–SBA-15 and Salophen-MnCl@{NH_2}–SBA-15 materials contain *c.a.* 0.2 mmol g^{-1} of salophen complex but also *c.a.* 2.1 mmol g^{-1} of free aminopropyl groups. Working with {NH_2}–SBA-15 (without any Salen) and $^{n-}Bu_4NBr$ alone, all other reaction parameters being unchanged (especially the number of amino groups), also led to a nearly complete conversion after 24 h. Such blank test emphasized the non-innocent character of the free amino groups in Salophen-Ni@{NH_2}–SBA-15 and Salophen-MnCl@{NH_2}–SBA-15 materials since the results with $^{n-}Bu_4NBr$/{NH_2}–SBA-15 (Table 2, entry 8) turned out to be systematically better than those obtained with $^{n-}Bu_4NBr$ alone (Table 2, entry 1). Using Salophen-Ni@{NH_2}–SBA-15 and Salophen-MnCl@{NH_2}–SBA-15, the effect of the metal complexes turned out to be significant after the first 3 h, since a complete epoxide conversion was obtained after 7 h of reaction with both supported Ni and Mn co-catalysts, while the epoxide consumption, in their absence, was equal to 86% (Table 2, entry 9). Such positive influence of the free amino groups on the support was more easily observed when using Salophen-Ni due to its lower intrinsic efficiency shown in homogeneous conditions (Table 2, entry 2). Improvement of the catalytic activity of silica-supported compared to soluble phosphonium halides in CO_2 cycloaddition has already been observed.[60] In that case, the proposed explanation invoked a possible activation of the epoxide towards the halide attack owing to hydrogen bonding of the oxirane with the surface silanol groups of the support, thus playing the role of electrophilic sites. At first glance, one explanation in our case would be that similar activation of the epoxide could also occur through hydrogen

bonding between the free aminopropyl groups of the support and styrene oxide even if the N–H bond in $-(CH_2)_3-NH_2$ is less polar than the O–H bond in $\equiv$Si–OH. A beneficial effect due the presence of such groups able to form hydrogen bonding has also been emphasized in other works.[61–64] More generally, this behaviour is reminiscent of the anchoring mechanisms of substrates in the cavity of certain enzymes such as acetylcholinesterase.[65] Indeed, this cavity which typically consists in a region particularly rich in {NH} amides or positively charged residues allows for insertion or positioning of a substrate and actually works as a Lewis acid site useful for activation. Another explanation for the positive effect of the functionalized support would be due to the activation of CO_2 itself by the primary amine in $\{NH_2\}$–SBA-15, Salophen-Ni@$\{NH_2\}$–SBA-15 or Salophen-MnCl@$\{NH_2\}$–SBA-15 even if the resulting carbamate is not the promptest to transfer CO_2 to the anionic intermediate obtained from the attack of styrene oxide by bromide.[66] Usually activated carbamates issued from tertiary amines are preferred as exemplified in the work of J. Gao *et al.*[67] who reported a significant cyclocarbonate yield increase upon the addition of triethylamine. Nevertheless, some groups have reported the beneficial impact of primary amine auxiliaries in the design of homogeneous[62] or even heterogeneous catalysts[66,68] for the CO_2 addition onto epoxides.

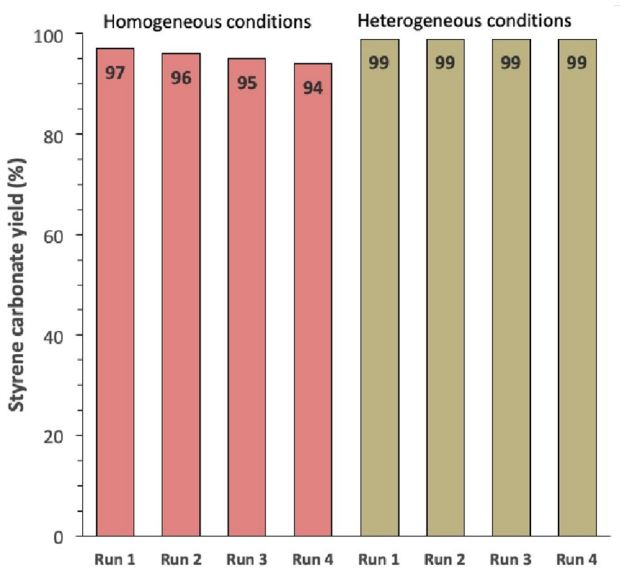

Figure 9. Styrene carbonate yield (%) for Salophen-MnCl (3) (homogeneous conditions, in light red) after 1 to 4 runs of 3 h and for Salophen-Ni@$\{NH_2\}$–SBA-15 (heterogeneous conditions, in light green) after 1 to 4 runs of 23 h. Conditions: Styrene oxide (6.1 mmol), $^{n-}Bu_4NBr$ (0.1 mmol), homogeneous or supported Salophen-M (0.05 mmol) in 13.3 mL of benzonitrile at 120 °C under 15 bars of CO_2.

2.3.3. Stability of the catalysts

Finally, the stability of the co-catalysts was investigated in homogeneous conditions with Salophen-MnCl (**3**) (4 runs of 3 h with styrene oxide and CO_2 replenishment without any work-up) and in heterogeneous conditions with Salophen-Ni@$\{NH_2\}$–SBA-15 (4 runs of 23 h separated by filtration and drying steps). The detailed operating protocols for both experiments were based on the optimized experimental conditions described in the experimental part and in Table 2 (see experimental section for details), and the results are displayed in Figure 9. In these experiments, both co-catalysts were successfully re-used without any appreciable loss of performance after respectively four cycles, leading to a nearly complete styrene conversion (from 94 to 99%) in all cases, thus indicating an excellent stability in homogeneous and heterogeneous conditions.

Furthermore, the supported catalyst Salophen-Ni@$\{NH_2\}$–SBA-15 could be characterized after the catalytic process in order to verify that the integrity of the metal complexe is maintained. For sake of illustration, the Raman spectra of Salophen-Ni@$\{NH_2\}$–SBA-15 were compared before and after 4 catalytic cycles (see supporting information Figure S8), showing the same patterns in both cases. In addition, the comparison of the textural parameters of Salophen-Ni@$\{NH_2\}$–SBA-15 before and after 4 catalytic cycles (Figure 8 and Table 1) also demonstrated that the catalytic materials were also not altered at the microscale level. Indeed, mean pore diameter values before and after catalysis were shown to be almost unchanged while the BET surface areas and pore volumes turned out to be equivalent.

3. Conclusion

In this study, nickel(II) and manganese (III) complexes with the *N,N′*-bis(3,5-di-*tert*-butylsalicylidene)-1-carboxy-3,4-phenylene-diamine (Salophen-MnCl and Salophen-Ni), bearing carboxylic acid groups on their ligands, were synthesized and fully characterized. Both were shown to work as $^{n-}Bu_4NBr$ co-catalyst for the cycloaddition of CO_2 onto styrene oxide, thus affording a real added value in terms of epoxide conversion (100% after 3 h of reaction at 120 °C under 15 bar of CO_2 with Salophen-MnCl instead of 62% without). In addition, the soluble Salophen-MnCl/$^{n-}Bu_4NBr$ system proved to be stable after 3 successive replenishments of the consumed styrene oxide.

Using DCC as a convenient and efficient coupling agent, Salophen-MnCl and Salophen-Ni were easily heterogenized, with up to 1 wt.% of metal at once, by amide linkage onto a SBA-15 silica bearing propylamine groups, thus affording recoverable co-catalysts. Immobilization of the less active complex in solution, Salophen-Ni, even resulted in an enhanced co-catalytic activity (100% conversion of styrene oxide after 7 h instead of 85% in solution). This particular result paves thus the way to the utilization of (rarely used in the literature) Ni^{2+} catalysts for the CO_2 cycloaddition onto epoxides. Furthermore, the heterogenized form of Salophen-Ni was successfully re-used without any appreciable loss of activity over 4 runs. In addition, the preservation of the

integrity of this co-catalyst, after the catalytic process, was demonstrated by Raman spectroscopy as well as by the measurement of the N_2 desorption/absorption isotherms.

More important, this study also showed that propylamine functions at the surface of the {NH_2}–SBA-15 support alone play also a co-catalytic role for the CO_2 cycloaddition reaction in the presence of $^{n-}Bu_4Br$ and give rise to some synergy when using covalently grafted Salophen-Ni and $^{n-}Bu_4Br$. In both cases, the origin of this effect would be due to the activation of the epoxide and/or of CO_2. In conclusion, it is clear that this work is only a first step towards a completely heterogeneous catalytic system, in which the tetraalkylammonium halide catalyst and the metal-salophen co-catalyst will both be covalently anchored on the same support. However, this work is currently in progress and will be the subject of a second manuscript.

Experimental Section

Synthesis and heterogenization of the precursor complexes

Preparation of *N,N′*-bis(3,5-di-*tert*-butylsalicylidene)-1-carboxy-3,4-phenylene-diamine-nickel(II) (Salophen-Ni (2)). H_2Salophen ligand (**1**) (1.000 g, 1.70 mmol, see preparation in Supporting Information and characterization in Figure S1 (HRMS spectrum) and Figure S2 (^{1}H NMR spectrum)) was dissolved in 50 mL of dry methanol under argon in a two-neck round-bottom flask connected to a condenser. A solution of $NiCl_2.6H_2O$ in excess (1.069 g, 4.50 mmol) dissolved in 30 mL of dry methanol was then added and the mixture was refluxed for one hour under argon. The volume of the solution was then reduced until 20 mL under vacuum and allowed to stand at room temperature overnight. The dark red solid (Salophen-Ni (**2**)) that appeared during this time was then filtered at air on a frit glass (n°4) and washed quickly with small portions of methanol, yielding 0.550 g (51 %). ^{1}H NMR ([D_6] dmso, ppm, Figure S3): δH 8.98 (1H, s, C(7)H=N), 8.91 (1H, s, C(7′)H=N), 8.72 (1H, s, C(12)H), 8.27 (1H, d, $^3J_{HH}$ = 12.0 Hz, C(9)H), 7.84 (1H, d, $^3J_{HH}$ = 12.0 Hz, C(10)H), 7.63 (1H, d, $^4J_{HH}$ = 3.3 Hz, C(6)H), 7.49 (1H, d, ^{4}JHH = 2.6 Hz, C(6′)H), 7.38 (1H, d, ^{4}JHH = 3.3 Hz, C(4)H), 7.35 (1H, d, ^{4}JHH = 2.6 Hz, C(4′)H), 1.41 (18H, s, C(3)C$(CH_3)_3$ + C(3′)C$(CH_3)_3$), 1.30 (18H, s, C(5)C$(CH_3)_3$) + C(5′)C$(CH_3)_3$); IR (KBr, cm^{-1}): 3422 (m), 3054(m), 2959 (s), 1729 (s), 1686 (m), 1619 (s), 1579 (s), 1523 (s), 1458 (m), 1426 (s), 1386 (s), 1359 (s), 1260 (m), 1200 (s), 1180 (s), 1130 (m), 1026 (m), 788 (m), 541 (m). HRMS [**2**-H]$^-$ (ESI): m/z = 639.27 (Figure S4).

Preparation of *N,N′*-bis(3,5-di-*tert*-butylsalicylidene)-1-carboxy-3,4-phenylene-diamine-chloro-Manganese(III) (Salophen-MnCl (3)). H_2Salophen ligand (1) (0.347 g, 0.60 mmol) was dissolved in 20 mL of dry THF under argon in a two-neck round-bottom flask connected to a condenser. [$MnCl_2(THF)_2$] (0.160 g, 0.60 mmol) was then added to the solution and the mixture was stirred at room temperature for 1 h, then refluxed for 20 min. After cooling at room temperature, triethylamine (0,12 g, 1.20 mmol, 0,17 mL) was then added and the mixture stirred for another 45 min. The volume of the solution was then reduced up to 10 mL under vacuum and allowed to stand at room temperature overnight. After this period, a white powder (triethylammonium chloride) was filtered and discarded. The brown solution was evaporated, leading to a brown solid (Salophen-MnCl (3)) that can be recrystallized in THF (yield: 0.350 g, 0,50 mmol, 88 %). IR (KBr, cm^{-1}): 3416 (m), 2958 (m), 1680 (sh), 1610 (s), 1573 (s), 1466 (s), 1392 (s), 1361 (s), 1325 (s), 1249 (s), 1198 (s), 1178 (s), 1097 (s), 1026 (s), 807 (s), 781 (s), 548 (m). HRMS [3-Cl]$^+$ (ESI) : m/z = 637.28 (Figure S5).

Covalent grafting of Salophen-Ni (2) onto {NH_2}–SBA-15. {NH_2}–SBA-15 (0.30 g, [–RNH_2] = 2.3 mmol g^{-1}, corresponding to 0.69 mmol of {–RNH_2} functions, see synthesis in SI) and Salophen-Ni (**2**) (0.105 g, 0.16 mmol) were dried under vacuum overnight in two schlenk tubes. Then, Salophen-Ni (**2**) was dissolved in dichloromethane (DCM, 3 mL). In parallel, 1-hydroxy-1H-benzotriazole (HOBT, 0.007 g, 0.05 mmol) and *N,N′*-dicyclohexylcarbodiimide (DCC, 0.05 g, 0.22 mmol) were dissolved in 2 mL of DCM and the resulting solution was added to the solution of **2**. The mixture was stirred for 40 min at room temperature. Meanwhile, 10 mL of DCM were added to {NH_2}–SBA-15. After 40 min, the previous mixture of **2**, HOBT and DCC was transferred to the suspension of {NH_2}–SBA-15 and refluxed for 6 h under N_2. Then, the solvent was evaporated until dryness and the resulting red powder was washed successively with refluxing methanol and acetone using a Soxhlet, respectively for 3 days and 24 h. Salophen-Ni@{NH_2}–SBA-15 (0.32 g) was thus obtained as a dark red purple powder (Ni%$_{weight}$ = 1.30 % determined by TGA (10.3 % mol Ni/mol –NH_2) corresponding to a Ni grafting yield of 52 %).

Covalent grafting of Salophen-MnCl (3) onto {NH_2}–SBA-15. {NH_2}–SBA-15 (1.5 g, [–RNH_2] = 2.3 mmol g^{-1}, corresponding to 3.45 mmol of {–RNH_2} functions) and Salophen-MnCl (**3**) (0.30 g, 0.45 mmol) were dried under vacuum overnight in two schlenk tubes. Then, Salophen-MnCl (**3**) was dissolved in DCM, 6 mL, and 1-hydroxy-1H-benzotriazole (0.021 g, 0.138 mmol) and N,N′-dicyclohexylcarbodiimide (DCC, 0.135 g, 0.66 mmol) were added to this solution. The mixture was stirred for 40 min at room temperature. Meanwhile, 10 mL of DCM were added to {NH_2}–SBA-15. After 40 min, the previous mixture of **3**, HOBT and DCC was transferred to the suspension of {NH_2}–SBA-15 and refluxed for 6 h under N_2. The solvent was then evaporated until dryness and the resulting brown powder was washed successively with refluxing methanol and acetone using a Soxhlet, respectively for 3 days and 24 h. Salophen-MnCl@{NH_2}–SBA-15 (1.44 g) was thus obtained as a dark brown powder (Mn %$_{weight}$ = 1.03 % determined by TGA (8.2 % mol Mn/mol –NH_2) corresponding to a Mn grafting yield of 68 %).

Protocols for the catalysis tests

After each catalytic test, the resulting solutions or suspensions were analysed by gas chromatography (GC, see details in Supporting Information) after dilution (samples of 25 µL diluted in 10 mL of CH_2Cl_2).

Experiments in homogeneous conditions (including stability test). In a 50 mL Teflon container, 0.7 mL of styrene oxide (6.1 mmol) and 0.031 g (0.100 mmol) of $^{n-}Bu_4NBr$ were dissolved in 13.3 mL of benzonitrile. Except for the tests performed in the absence of co-catalysts, 0.031 g of Salophen-Ni (or 0.033 g Salophen-MnCl) (0.05 mmol)) was added and the resulting mixture was stirred for 5 min at room temperature. Then, the autoclave was pressurized at 11 bar of CO_2 (corresponding to 41 mmol). The temperature was then increased up to 120 °C in 40 min, leading to a CO_2 pressure of 15 bar. Heating was then prolonged for 3, 7 or 23 h and the reaction was quenched by cooling the autoclave into a water-ice mixture.

For the stability test, the reaction was carried out for 3 h, then quenched as described above. After analysis by GC, a new batch of styrene oxide (0.7 mL, 6.1 mmol) was introduced in the recovered Teflon container and the reaction mixture was stirred for 5 min at room temperature. Then, the autoclave was pressurized as described before. This procedure was repeated 3 times.

Experiments with the supported complexes (including recyclability test). The protocols were identical with the exception of the mass of co-catalysts added. 0.218 g of Salophen-Ni@{NH_2}–SBA-15 (or 0.259 g Salophen-MnCl@{NH_2}–SBA-15), corresponding to 0.05 mmol of immobilized metal salophen complexes, was suspended in the benzonitrile solution. Then, the autoclave was pressurized as described before. After 3, 7 or 23 h, the reaction was quenched by cooling the autoclave into a water-ice mixture, and the reaction mixture was filtered on a büchner funnel, in order to separate the supported catalyst.

For the recyclability test, the reaction was carried out for 23 h and the solid recovered after each attempt was carefully washed by acetone, dried in an oven at 50 °C for 12 h and weighted to check the mass after each run. This procedure was repeated three times.

Other synthesis procedures and all the details on the different characterization techniques are reported in the Supporting Information: HRMS (ESI) spectrum and ^{1}H NMR spectrum of H_2salophen ligand **1**, HRMS (ESI) spectrum and ^{1}H NMR spectrum of Salophen-Ni (**2**), HRMS (ESI) spectrum of Salophen-MnCl (**3**), scheme of the synthetic procedure for the preparation of {NH_2}–SBA-15, ^{13}C CP-MAS NMR spectra of Salophen-Ni and Salophen-Ni@{NH_2}–SBA-15, Nitrogen adsorption-desorption isotherms of Salophen-MnCl@{NH_2}–SBA-15 and Raman spectra of Salophen-Ni@{NH_2}–SBA-15 before and after 4 catalytic cycles.

Acknowledgements

This work benefited from the support of the project OxCyCat-CO_2 (ANR-17-CE06-0009) of the Agence Nationale de la Recherche (ANR) for a PhD fellowship to Mr Matthieu Balas, for financial reward for Mr Sébastien Beaudoin and more generally for funding this work. The authors want also to acknowledge the Centre National de la Recherche Scientifique (CNRS), Sorbonne Université, Mrs Delphine Talbot, from Laboratoire de Physicochimie des Electrolytes et Nanosystèmes Interfaciaux (PHENIX, UMR CNRS 8234, Sorbonne Université) for her help in atomic absorption measurements for Ni/Mn analyses and Mr Jean-Marc Krafft, from Laboratoire de Réactivité de Surface (LRS, UMR CNRS 7197, Sorbonne Université) for his help in Raman spectroscopy.

Conflict of Interest

The authors declare no conflict of interest.

Keywords: Cyloaddition · CO_2 valorization · Hybrid catalysts · Mesoporous materials · Salen derivatives

[1] A. W. Kleij, M. North, A. Urakawa, *ChemSusChem* **2017**, *10*, 1036–1038.
[2] M. North, *ChemSusChem* **2019**, *12*, 1763–1765.
[3] M. Aresta, *Coord. Chem. Rev.* **2017**, *334*, 150–183.
[4] M. Peters, B. Köhler, W. Kuckshinrichs, W. Leitner, P. Markewitz, T. E. Müller, *ChemSusChem* **2011**, *9*, 1216–1240.
[5] G. Laugel, C. Carvalho Rocha, P. Massiani, T. Onfroy, F. Launay, *Adv. Chem. Lett.* **2013**, *1*, 195–214.
[6] ■■■Dear author, please add authors■■■, *ChemSusChem* **2017**, *10*, 1034–1297.
[7] C. Chauvier, T. Cantat, *ACS Catal.* **2017**, *7*, 2107–2115.
[8] S. Sopeña, G. Fiorani, C. Martín, A. W. Kleij, *ChemSusChem* **2015**, *8*, 3248–3254.
[9] M. Cokoja, M. E. Wilhelm, M. H. Anthofer, W. A. Herrmann, F. E. Kühn, *ChemSusChem* **2015**, *8*, 2436–2454.
[10] M. Alves, B. Grignard, S. Gennen, C. Detrembleur, C. Jerome, T. Tassaing, *RSC Adv.* **2015**, *5*, 53629–53636.
[11] Z. Z. Yang, L. N. He, C. X. Miao, S. Chanfreau, *Adv. Synth. Catal.* **2010**, *352*, 2233–2240.
[12] Y. Zhou, S. Hu, X. Ma, S. Liang, T. Jiang, B. Han, *J. Mol. Catal. A* **2008**, *284*, 52–57.
[13] B. Chatelet, L. Joucla, J. P. Dutasta, A. Martinez, K. C. Szeto, V. Dufaud, *J. Am. Chem. Soc.* **2013**, *135*, 5348–5351.
[14] C. Miceli, J. Rintjema, E. Martin, E. C. Escudero-Adán, C. Zonta, G. Licini, A. W. Kleij, *ACS Catal.* **2017**, *7*, 2367–2373.
[15] D. Darensbourg, *Chem. Rev.* **2007**, *107*, 2388–2410.
[16] P. Lan, L. E. White, E. S. Taher, P. E. Guest, M. G. Banwell, A. C. Willis, *J. Nat. Prod.* **2015**, *78*, 1963–1968.
[17] X. Xiaoding, J. A. Moulijn, *Energy Fuels* **1996**, *10*, 305–325.
[18] J. Melendez, M. North, R. Pasquale, *Eur. J. Inorg. Chem.* **2007**, 3323–3326.
[19] X. Zhang, Y. B. Jia, X. B. Lu, B. Li, H. Wang, L. C. Sun, *Tetrahedron Lett.* **2008**, *49*, 6589–6592.
[20] J. Rintjema, L. P. Carrodeguas, V. Laserna, S. Sopena, A. W. Kleij, *Top. Organomet. Chem.* **2016**, *53*, 39–71.
[21] L. Cuesta-Aluja, A. Campos-Carrasco, J. Castilla, M. Reguero, A. M. Masdeu-Bulto, A. Aghmiz, *J. CO2 Util.* **2016**, *16*, 10–22.
[22] J. W. Comerford, I. D. V. Ingram, M. North, X. Wu, *Green Chem.* **2015**, *17*, 1966–1987.
[23] M. Aresta, A. Dibenedetto, *Dalton Trans.* **2007**, 2975–2992.
[24] A. Kamphuis, F. Picchioni, P. P. Pescarmona, *Green Chem.* **2019**, *21*, 406–448.
[25] M. Alves, B. Grignard, R. Mereau, C. Jerome, T. Tassaing, C. Detrembleur, *Catal. Sci. Technol.* **2017**, *7*, 2651–2684.
[26] A. Mirabaud, J.-C. Mulatier, A. Martinez, J.-P. Dutasta, V. Dufaud, *Catal. Today* **2017**, *281*, 387–391.
[27] C. Carvalho Rocha, T. Onfroy, J. Pilme, A. Denicourt-Nowicki, A. Roucoux, F. Launay, *J. Catal.* **2016**, *333*, 29–39.
[28] L. Cuesta-Aluja, M. Djoufak, A. Aghmiz, R. Rivas, L. Christ, A. Masdeu-Bulto, *J. Mol. Catal. A* **2014**, *381*, 161–170.
[29] M. Djoufak, *PhD thesis*, dir. L. Christ, University of Lyon **2013**.
[30] T. Ema, Y. Miyazaki, S. Koyama, Y. Yano, T. Sakai, *Chem. Commun.* **2012**, *48*, 4489–4491.
[31] J. A. Castro-Osma, K. J. Lamb, M. North, *ACS Catal.* **2016**, *6*, 5012–5025.
[32] J. Melendez, M. North, P. Villuendas, C. Young, *Dalton Trans.* **2011**, *40*, 3885–3902.
[33] P. A. Carvalho, J. W. Comerford, K. J. Lamb, M. North, P. S. Reiss, *Adv. Synth. Catal.* **2019**, *361*, 345–354.
[34] S. Wei, Y. Tang, G. Xu, X. Tang, Y. Ling, R. Li, Y. Sun, *React. Kinet. Catal. Lett.* **2009**, *97*, 329–333.
[35] A. Heckel, D. Seebach, *Helv. Chim. Acta* **2002**, *85*, 913–926.
[36] S. Xiang, Y. Zhang, Q. Xin, C. Li, *Chem. Commun.* **2002**, 2696–2697.
[37] H. Zhang, S. Xiang, J. Xiao, C. Li, *J. Mol. Catal. A* **2005**, *238*, 175–184.
[38] L. Saikia, D. Srinivas, P. Ratnasamy, *Microporous Mesoporous Mater.* **2007**, *104*, 225–235.
[39] G. Trusso Sfrazzetto, S. Millesi, A. Pappalardo, R. M. Toscano, F. P. Ballistreri, G. A. Tomaselli, A. Gulino, *Catal. Sci. Technol.* **2015**, *5*, 673–679.
[40] F. Bentaleb, O. Makrygenni, D. Brouri, C. Coelho Diogo, A. Mehdi, A. Proust, F. Launay, R. Villanneau, *Inorg. Chem.* **2015**, *54*, 7607–7616.
[41] O. Makrygenni, D. Brouri, A. Proust, F. Launay, F. Launay, R. Villanneau, *Microporous Mesoporous Mater.* **2019**, *278*, 314–321.
[42] T. Luts, R. Frank, W. Suprun, S. Fritzsche, E. Hey-Hawkins, H. Papp, *J. Mol. Catal. A* **2007**, *273*, 250–258.
[43] T. Luts, H. Papp, *Kinet. Catal.* **2007**, *48*, 176–182.
[44] F. Jutz, J.-D. Grunwaldt, A. Baiker, *J. Mol. Catal. A* **2009**, *297*, 63–72.
[45] J. L. S. Milani, A. M. Meireles, B. N. Cabral, W. de A Bezerra, F. T. Martins, D. Carvalho da Silva Martins, R. Pavao das Chagas, *J. CO2 Util.* **2019**, *30*, 100–106.
[46] L. Cuesta-Aluja, J. Castilla, A. M. Masdeu-Bulto, C. A. Henriques, M. J. F. Calvete, M. M. Pereira, *J. Mol. Catal. A* **2016**, *423*, 489–494.
[47] R. Srivastava, T. H. Bennur, D. Srinivas, *J. Mol. Catal. A* **2005**, *226*, 199–205.
[48] Y. Fan, J. Li, Y. Ren, H. Jiang, *Eur. J. Inorg. Chem.* **2017**, *43*, 4982–4989.
[49] F. Chiker, F. Launay, J. P. Nogier, J. L. Bonardet, *Appl. Catal. A* **2003**, *243*, 309–321.

[50] M. Boutros, G. Shirley, T. Onfroy, F. Launay, *Appl. Catal. A* **2011**, *394*, 158–165.
[51] R. Villanneau, A. Marzouk, Y. Wang, A. Ben Djamaa, G. Laugel, A. Proust, F. Launay, *Inorg. Chem.* **2013**, *52*, 2958–2965.
[52] M. Schley, S. Fritzsche, P. Lönnecke, E. Hey-Hawkins, *Dalton Trans.* **2010**, *39*, 4090–4106.
[53] M. Datta, D. H. Brown, W. E. Smith, *Spectrochim. Acta Part A* **1983**, *39*, 37–41.
[54] T. A. de Toledo, P. S. Pizani, L. E. da Silva, A. M. R. Teixeira, P. T. C. Freire, *J. Mol. Struct.* **2015**, *1097*, 106–111.
[55] S. Foltran, J. Alsarraf, F. Robert, Y. Landais, E. Cloutet, H. Cramail, T. Tassaing, *Catal. Sci. Technol.* **2013**, *3*, 1046–1055.
[56] C. Baleizão, B. Gigante, M. J. Sabater, H. Garcia, A. Corma, *Appl. Catal. A* **2002**, *228*, 279–288.
[57] M. Ramin, F. Jutz, J.-D. D. Grunwaldt, A. Baiker, *J. Mol. Catal. A* **2005**, *242*, 32–39.
[58] M. Alvaro, C. Baleizao, D. Das, E. Carbonell, H. García, *J. Catal.* **2004**, *228*, 254–58.
[59] F. Jutz, J. D. Grunwaldt, A. Baiker, *J. Mol. Catal. A* **2008**, *279*, 94–103.
[60] T. Takahashi, T. Watahiki, S. Kitazume, H. Yasuda, T. Sakakura, *Chem. Commun.* **2006**, 1664–1666.
[61] L.-Q. Wei, B.-H. Ye, *Inorg. Chem.* **2019**, *58*, 4385–4393.
[62] T. Werner, N. Tenhumberg, *J. CO2 Util.* **2014**, *7*, 39–45.
[63] J. Liang, Y.-B. Huang, R. Cao, *Coord. Chem. Rev.* **2019**, *378*, 32–65.
[64] M. Liu, X. Wang, Y. Jiang, J. Sun, M. Arai, *Catal. Rev. Sci. Eng.* **2019**, *61*, 214–269.
[65] Y. Zhang, J. Kua, J. A. McCammon, *J. Am. Chem. Soc.* **2002**, *124*, 10572–10577.
[66] R. Srivastava, D. Srinivas, P. Ratnasamy, *Microporous Mesoporous Mater.* **2006**, *90*, 314–326.
[67] J. Gao, L. li, C. Cui, M. A. Ziaee, Y. Gong, R. Sa, H. Zhong, *RSC Adv.* **2019**, *9*, 13122–13127.
[68] Y. Li, X. Zhang, J. Lan, P. Xu, J. Sun, *Inorg. Chem.* **2019**, *58*, 13917–13926.

Manuscript received: February 18, 2021
Revised manuscript received: March 15, 2021

FULL PAPERS

Ni^{II} and Mn^{III} Schiff base complexes bearing a pending carboxylic group were grafted onto a mesoporous amino-functionalized SBA-15 silica. The co-catalytic behaviour of the grafted complexes with $^{n-}Bu_4NBr$ was evaluated in the CO_2 cycloaddition onto styrene oxide. Upon immobilization at the surface of the SBA-15, the performances of the Ni^{2+} complex were enhanced, hence highlighting a synergistic effect with the amine functions of the support.

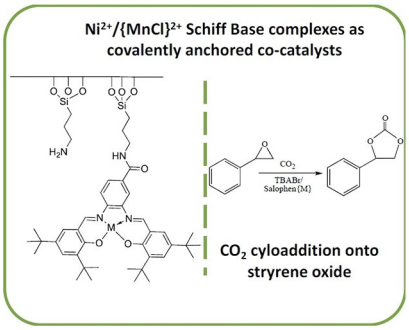

M. Balas, S. Beaudoin, Prof. A. Proust, Prof. F. Launay, Dr. R. Villanneau**

Launay, Villanneau and co-workers investigate the catalytic properties of nickel(II) and manganese(II) Schiff base complexes @ipcm_sorbonne

Share your work on social media! *EurJIC* has added Twitter as a means to promote your article. Twitter is an online microblogging service that enables its users to send and read short messages and media, known as tweets. Please check the pre-written tweet in the galley proofs for accuracy. If you, your team, or institution have a Twitter account, please include its handle @username. Please use hashtags only for the most important keywords, such as #catalysis, #nanoparticles, or #proteindesign. The ToC picture and a link to your article will be added automatically, so the **tweet text must not exceed 250 characters**. This tweet will be posted on the journal's Twitter account (follow us @EurJIC) upon publication of your article in its final (possibly unpaginated) form. We recommend you to re-tweet it to alert more researchers about your publication, or to point it out to your institution's social media team.

ORCID (Open Researcher and Contributor ID)

Please check that the ORCID identifiers listed below are correct. We encourage all authors to provide an ORCID identifier for each coauthor. ORCID is a registry that provides researchers with a unique digital identifier. Some funding agencies recommend or even require the inclusion of ORCID IDs in all published articles, and authors should consult their funding agency guidelines for details. Registration is easy and free; for further information, see http://orcid.org/.

Matthieu Balas
Sébastien Beaudoin
Prof. Anna Proust
Prof. Franck Launay
Dr. Richard Villanneau http://orcid.org/0000-0003-1465-3494